Radiation and Porosity Effects on the Magnetohydrodynamic Flow Past an Oscillating Vertical Plate with Uniform Heat Flux

Samiulhaq[a], Constantin Fetecau[b], Ilyas Khan[a], Farhad Ali[a], and Sharidan Shafie[a]

[a] Department of Mathematical Sciences, Faculty of Science, Universiti Teknologi Malaysia, 81310 UTM Skudai, Malaysia

[b] Academy of Romanian Scientists, 050094 Bucuresti, Romania

Reprint requests to S. Shafie.; E-mail: ridafie@yahoo.com

Z. Naturforsch. **67a,** 572 – 580 (2012) / DOI: 10.5560/ZNA.2012-0070
Received May 24, 2012 / published online September 19, 2012

Magnetohydrodynamic free convection flow of an incompressible viscous fluid past an infinite vertical oscillating plate with uniform heat flux in a porous medium is studied. Exact dimensionless solutions of momentum and energy equations, under Boussinesq approximation, are obtained using Laplace transforms. They satisfy all imposed initial and boundary conditions and reduce to known solutions from the literature as special cases. Finally, the influence of different parameters like thermal radiation parameter, Grashof number, Prandtl number, and time on velocity, temperature, and skin friction is shown by graphs.

Key words: Magnetohydrodynamic Flow; Oscillating Vertical Plate; Thermal Radiation; Porous Medium.

1. Introduction

Free convection flows of an incompressible viscous fluid past a vertical infinite plate were extensively studied in the literature due to their vast applications in engineering and environmental processes. They are also of great interest in industrial applications such as fiber and granular insulation, geothermal systems, filtration processes, nuclear reactors, design of spaceship, etc. Unsteady free convection flow past a moving vertical plate is investigated by many researchers considering different thermal conditions on the boundary. Soundalgekar [1] seems to be the first who provided an exact solution for free convection effects on the flow of a viscous incompressible fluid past an impulsively started infinite vertical plate. Later, Raptis and Singh [2] studied the free-convection flow of a visco-elastic fluid past an accelerated vertical plate. The effects of magnetic field have been also taken into consideration. Free convection effects on the flow past an exponentially accelerated vertical plate was studied by Singh and Kumar [3]. Free convection oscillating flow past an infinite vertical porous plate with constant suction were studied by Soundalgekar [4]. Mansour [5] studied the interaction of free convection with thermal radiation of the oscillating flow past a vertical plate. An interesting study of the effects of thermal radiation on the flow past an infinite vertical oscillating isothermal plate in the presence of a transversely applied magnetic field has been recently realized by Chandrakala and Bhaskar [6]. The effects of thermal radiation on the boundary layer flow over a horizontal plate have been also studied by Ishak [7, 8].

In the last years, problems of free convection and heat transfer flows through porous media under the influence of a magnetic field have attracted the attention of many researchers. This type of flows has applications in magnetohydrodynamic (MHD) power generation, MHD pumps, flowmeters and accelerators, plasma studies, nuclear reactor using liquid metal coolant, and geothermal energy extraction. On the other hand, flows by a porous medium have numerous engineering and geophysical applications in chemical engineering for filtration and purification process, agriculture engineering to study the underground water resources, and petroleum technology to study the movement of natural gas, oil, and water through oil reservoirs. Among the most recent and interesting results from this area, we remember here the work by Rajesh and Varma [9], Narahari and Ishak [10], Seth et al. [11], Chandrakala and Bhaskar [12] and Chandrakala [13].

Having in mind the above remarks regarding the importance of magnetic and porous effects on the fluid motion, we study the effect of a uniform transverse magnetic field on the free convection of an incompressible viscous fluid past an infinite vertical oscillating plate with uniform heat flux in a porous medium. The dimensionless governing equations are solved using the Laplace transform technique, and exact solutions for velocity and temperature are obtained in terms of exponential and complementary error functions. Knowing the velocity, the dimensionless expression of the skin friction is also determined. In the absence of radiation effects, the expression of the temperature reduces to that obtained by Chaudhary et. al. [14, Eq. (15)] and the solution for velocity agree well with [14, Eq. (16)] of the same reference. Some special cases are considered, and in the absence of thermal, magneto, and porous effects the solution obtained by Erdogan [15, Eq. (8)] is recovered for velocity. Finally, the effects of pertinent parameters on velocity, temperature, and skin friction are graphically underlined.

2. Statement of the Problem and Solution

Let us consider an incompressible electrically conducting viscous fluid past an infinite vertical plate embedded in a porous medium. A magnetic field of uniform strength B_0 is transversely applied to the plate. The induced magnetic field due to the fluid motion is assumed to be negligible in comparison to the applied magnetic field. This restriction is justified for metallic liquids and partially ionized fluids [16] because their magnetic Reynolds number is very small. The effect of polarization of the fluid is also negligible as no external electric field is applied. At initial moment $t = 0$, both the plate and the fluid are at rest at the constant temperature T_∞. At time $t = 0^+$, the plate begins to oscillate in its plane $(y = 0)$ according to

$$v = U\cos(\omega t)\boldsymbol{i}\,,\quad t > 0, \tag{1}$$

where the constant U is the amplitude of the motion, $\boldsymbol{i}$ is the unit vector in the flow direction, and ω is the frequency of vibrations. Due to the shear, the fluid is gradually moved, and its velocity is of the form

$$v = v(y,t) = u(y,t)\boldsymbol{i}\,.$$

In view of the above assumptions, as well as of the usual Boussinesq's approximation, the governing equations reduce to Seth et al. [11, Eqs. (1) and (2)]

$$\frac{\partial u}{\partial t} = \nu\frac{\partial^2 u}{\partial y^2} - \frac{\sigma B_0^2}{\rho}u - \frac{\nu}{K}u + g\beta\,(T - T_\infty)\,, \tag{2}$$

$$\frac{\partial T}{\partial t} = \frac{k}{\rho c_\mathrm{p}}\frac{\partial^2 T}{\partial y^2} - \frac{1}{\rho c_\mathrm{p}}\frac{\partial q_\mathrm{r}}{\partial y}\,, \tag{3}$$

where $T, \nu, \rho, \sigma, K, g, \beta, k, c_\mathrm{p}$, and q_r are, respectively, temperature of the fluid, kinematic viscosity, fluid density, electrical conductivity, permeability of porous medium, acceleration due to gravity, volumetric coefficient of thermal expansion, thermal conductivity, specific heat at constant pressure, and the radiative heat flux in y-direction.

Assuming that no slipping occurs between the plate and the fluid, the appropriate initial and boundary conditions of the system of partial differential equations (2) and (3) are

$$\begin{aligned} &u(y,0) = 0\,,\ \ T(y,0) = T_\infty \quad \text{for } y \geq 0\,,\\ &u(0,t) = U\cos(\omega t)\,,\ \ \frac{\partial T(0,t)}{\partial y} = -\frac{q}{k} \quad \text{for } t > 0\,,\\ &u \to 0 \ \ \text{and } T \to T_\infty \text{ as } y \to \infty\,,\ \ t > 0\,, \end{aligned} \tag{4}$$

where q is the constant heat flux. In the following, we adopt the Rosseland approximation for radiative flux q_r [10, 11, 13, 17], namely

$$q_\mathrm{r} = -\frac{4\sigma^*}{3\kappa^*}\frac{\partial T^4}{\partial y}\,, \tag{5}$$

where σ^* is the Stefan–Boltzmann constant and κ^* is the mean absorbtion coefficient. Assuming small temperature difference between the fluid temperature T and the free stream temperature T_∞, expanding in Taylor series T^4 about T_∞, and neglecting the second and higher order terms, we find that

$$T^4 \cong 4T_\infty^3 T - 3T_\infty^4\,. \tag{6}$$

It is worth pointing out that (6), expressing the term T^4 as a linear function, is widely used in computational fluid dynamics involving radiation absorbtion problems [18].

Introducing (6) into (3), we obtain (see also Seth et al. [11, Eq. (6)])

$$\rho c_\mathrm{p}\frac{\partial T}{\partial t} = k\frac{\partial^2 T}{\partial y^2} + \frac{16\sigma^* T_\infty^3}{3\kappa^*}\frac{\partial^2 T}{\partial y^2}\,. \tag{7}$$

Now using the next dimensionless quantities

$$\begin{aligned} &u^* = \frac{u}{U},\ y^* = \frac{U}{\nu}y,\ t^* = \frac{U^2}{\nu}t,\\ &\omega^* = \frac{\nu}{U^2}\omega,\ \theta = \frac{Uk}{\nu q}(T-T_\infty),\\ &\mathrm{Gr} = \left(\frac{\nu}{U^2}\right)^2 \frac{g\beta q}{k},\ \mathrm{Pr} = \frac{\mu c_\mathrm{p}}{k},\\ &N_\mathrm{r} = \frac{16\sigma^* T_\infty^3}{3k\kappa^*},\ M^2 = \frac{\sigma\nu B_0^2}{\rho U^2},\ K^* = \frac{U^2}{\nu^2}K, \end{aligned} \tag{8}$$

and dropping out the star notation from u, y, t, ω, and K, the governing equations (2) and (7) take the simplified forms

$$\begin{aligned} \frac{\partial u(y,t)}{\partial t} =& \frac{\partial^2 u(y,t)}{\partial y^2} - Hu(y,t)\\ &+ \mathrm{Gr}\theta(y,t);\ y,t>0, \end{aligned} \tag{9}$$

$$\mathrm{Pr}\frac{\partial \theta(y,t)}{\partial t} = (1+N_\mathrm{r})\frac{\partial^2\theta(y,t)}{\partial y^2};\ y,t>0, \tag{10}$$

where $H = M^2 + \frac{1}{K}$. In (8), Pr is the Prandtl number, Gr the Grashof number, and N_r the radiation parameter. In non-dimensional form, the initial and boundary conditions (4) become

$$\begin{aligned} &u(y,0) = 0,\ \theta(y,0) = 0 \quad \text{for } y \geq 0,\\ &u(0,t) = \cos(\omega t),\ \frac{\partial\theta(0,t)}{\partial y} = -1 \quad \text{for } t>0,\\ &u(y,t)\to 0,\ \theta(y,t)\to 0 \quad \text{as } y\to\infty \text{ and } t>0. \end{aligned} \tag{11}$$

The energy equation (10) is uncoupled to the momentum equation (9) and its solution with the corresponding initial and boundary conditions (11) was given by Das et al. [19, Eq. (10)] and Chandrakala [13, Eq. (11)]. Unfortunately, both results contain printing errors and the correct result is given by

$$\begin{aligned} \theta(y,t) =& \frac{2\sqrt{t}}{\sqrt{\mathrm{Pr}_\mathrm{eff}}}\\ &\cdot\left[\frac{1}{\sqrt{\pi}}\exp\left(-\frac{y^2\mathrm{Pr}_\mathrm{eff}}{4t}\right) - \frac{y\sqrt{\mathrm{Pr}_\mathrm{eff}}}{2\sqrt{t}}\,\mathrm{erf}\,c\left(\frac{y\sqrt{\mathrm{Pr}_\mathrm{eff}}}{2\sqrt{t}}\right)\right], \end{aligned} \tag{12}$$

where $\mathrm{Pr}_\mathrm{eff} = \frac{\mathrm{Pr}}{1+N_\mathrm{r}}$ is the effective Prandtl number as in Magyari and Pantokratoras [20]. Introducing (12) into (9), applying the Laplace transform with respect to t, and bearing in mind the initial and boundary conditions corresponding to the velocity $u(y,t)$, we find the solution

$$\begin{aligned} u(y,t) =& \frac{1}{4}\\ &\cdot\left[\mathrm{e}^{-\mathrm{i}\omega t}\left[\mathrm{e}^{-y\sqrt{H-\mathrm{i}\omega}}\,\mathrm{erf}\,c\left(\frac{y}{2\sqrt{t}} - \sqrt{(H-\mathrm{i}\omega)t}\right)\right.\right.\\ &\left.+\mathrm{e}^{y\sqrt{H-\mathrm{i}\omega}}\,\mathrm{erf}\,c\left(\frac{y}{2\sqrt{t}} + \sqrt{(H-\mathrm{i}\omega)t}\right)\right]\\ &+\mathrm{e}^{\mathrm{i}\omega t}\left[\mathrm{e}^{-y\sqrt{H+\mathrm{i}\omega}}\,\mathrm{erf}\,c\left(\frac{y}{2\sqrt{t}} - \sqrt{(H+\mathrm{i}\omega)t}\right)\right.\\ &\left.\left.+\mathrm{e}^{y\sqrt{H+\mathrm{i}\omega}}\,\mathrm{erf}\,c\left(\frac{y}{2\sqrt{t}} + \sqrt{(H+\mathrm{i}\omega)t}\right)\right]\right]\\ &+\frac{\mathrm{Gr}}{H\sqrt{\mathrm{Pr}_\mathrm{eff}}}\left[-\frac{1}{\pi}\left[\int_0^\infty \frac{\cos(y\sqrt{x})}{(x+H)^{\frac{3}{2}}}\left[1-\mathrm{e}^{-(x+H)t}\right]\mathrm{d}x\right.\right.\\ &\left.+\int_0^H \frac{\mathrm{e}^{-y\sqrt{x+H}}}{x^{\frac{3}{2}}}\left[1-\mathrm{e}^{-xt}\right]\mathrm{d}x\right]\\ &+\frac{\mathrm{e}^{bt}}{\pi}\left[\int_0^\infty \frac{\cos(y\sqrt{x})}{(x+H+b)\sqrt{x+H}}\left[1-\mathrm{e}^{-(x+H+b)t}\right]\mathrm{d}x\right.\\ &\left.+\int_0^H \frac{\mathrm{e}^{-y\sqrt{x+H}}}{(x+b)\sqrt{x}}\left[1-\mathrm{e}^{-(x+b)t}\right]\mathrm{d}x\right]\\ &+2\sqrt{\frac{t}{\pi}}\exp\left(-\frac{y^2\mathrm{Pr}_\mathrm{eff}}{4t}\right) - y\sqrt{\mathrm{Pr}_\mathrm{eff}}\,\mathrm{erf}\,c\left(\frac{y\sqrt{\mathrm{Pr}_\mathrm{eff}}}{2\sqrt{t}}\right)\\ &-\frac{\mathrm{e}^{bt}}{2\sqrt{b}}\left[\mathrm{e}^{-y\sqrt{b\mathrm{Pr}_\mathrm{eff}}}\,\mathrm{erf}\,c\left(\frac{y\sqrt{\mathrm{Pr}_\mathrm{eff}}}{2\sqrt{t}} - \sqrt{bt}\right)\right.\\ &\left.\left.-\mathrm{e}^{y\sqrt{b\mathrm{Pr}_\mathrm{eff}}}\,\mathrm{erf}\,c\left(\frac{y\sqrt{\mathrm{Pr}_\mathrm{eff}}}{2\sqrt{t}} + \sqrt{bt}\right)\right]\right], \end{aligned} \tag{13}$$

where the constant $b = \frac{H}{\mathrm{Pr}_\mathrm{eff}-1}$. The temperature $\theta(y,t)$ given in (12) is valid for all positive values of Pr_eff, while the solution for the velocity is not valid for $\mathrm{Pr}_\mathrm{eff} = 1$. Consequently, in this case, the velocity $u(y,t)$ has to be rederived starting from (9) and (10). The solution that is obtained for $\mathrm{Pr}_\mathrm{eff} = 1$, is

$$\begin{aligned} u(y,t) =& \\ &\frac{1}{4}\left[\mathrm{e}^{-\mathrm{i}\omega t}\left[\mathrm{e}^{-y\sqrt{H-\mathrm{i}\omega}}\,\mathrm{erf}\,c\left(\frac{y}{2\sqrt{t}} - \sqrt{(H-\mathrm{i}\omega)t}\right)\right.\right.\\ &\left.+\mathrm{e}^{y\sqrt{H-\mathrm{i}\omega}}\,\mathrm{erf}\,c\left(\frac{y}{2\sqrt{t}} + \sqrt{(H-\mathrm{i}\omega)t}\right)\right]\\ &+\mathrm{e}^{\mathrm{i}\omega t}\left[\mathrm{e}^{-y\sqrt{H+\mathrm{i}\omega}}\,\mathrm{erf}\,c\left(\frac{y}{2\sqrt{t}} - \sqrt{(H+\mathrm{i}\omega)t}\right)\right.\\ &\left.\left.+\mathrm{e}^{y\sqrt{H+\mathrm{i}\omega}}\,\mathrm{erf}\,c\left(\frac{y}{2\sqrt{t}} + \sqrt{(H+\mathrm{i}\omega)t}\right)\right]\right] \end{aligned}$$

$$+\frac{\mathrm{Gr}}{H}\left[-\frac{1}{\pi}\left[\int_0^\infty \frac{\cos(y\sqrt{x})}{(x+H)^{\frac{3}{2}}}\left[1-\mathrm{e}^{-(x+H)t}\right]\mathrm{d}x + \int_0^H \frac{\mathrm{e}^{-y\sqrt{x+H}}}{x^{\frac{3}{2}}}\left[1-\mathrm{e}^{-xt}\right]\mathrm{d}x\right] + 2\sqrt{\frac{t}{\pi}}\exp\left(-\frac{y^2}{4t}\right) - y\,\mathrm{erf}\,c\left(\frac{y}{2\sqrt{t}}\right)\right]. \quad (14)$$

The corresponding skin friction, which is a measure of the shear stress at the plate, can be determined by introducing (13) and (14) into

$$\tau = \tau(t) = -\left.\frac{\partial u(y,t)}{\partial y}\right|_{y=0}; \; t>0. \quad (15)$$

Its non-dimensional expressions are

$$\tau = \frac{\mathrm{e}^{-\mathrm{i}\omega t}}{2}\left[\sqrt{H-\mathrm{i}\omega}\,\mathrm{erf}\sqrt{(H-\mathrm{i}\omega)t} + \frac{1}{\sqrt{t\pi}}\mathrm{e}^{-(H-\mathrm{i}\omega)t}\right] + \frac{\mathrm{e}^{\mathrm{i}\omega t}}{2}\left[\sqrt{H+\mathrm{i}\omega}\,\mathrm{erf}\sqrt{(H+\mathrm{i}\omega)t} + \frac{1}{\sqrt{t\pi}}\mathrm{e}^{-(H+\mathrm{i}\omega)t}\right] + \frac{\mathrm{Gr}}{H\sqrt{\mathrm{Pr}_{\mathrm{eff}}}}\left[(1-\mathrm{e}^{bt})\sqrt{\mathrm{Pr}_{\mathrm{eff}}} - \frac{1}{\pi}\int_0^H \frac{\sqrt{H+x}}{x^{\frac{3}{2}}}\left[1-\mathrm{e}^{-tx}\right]\mathrm{d}x + \frac{\mathrm{e}^{bt}}{\pi}\int_0^H \frac{\sqrt{H+x}}{(b+x)\sqrt{x}}\left[1-\mathrm{e}^{-t(b+x)}\right]\mathrm{d}x\right], \quad (16)$$

for $\mathrm{Pr}_{\mathrm{eff}} \neq 1$ and

$$\tau = \frac{\mathrm{e}^{-\mathrm{i}\omega t}}{2}\left[\sqrt{H-\mathrm{i}\omega}\,\mathrm{erf}\sqrt{(H-\mathrm{i}\omega)t} + \frac{1}{\sqrt{t\pi}}\mathrm{e}^{-(H-\mathrm{i}\omega)t}\right] + \frac{\mathrm{e}^{\mathrm{i}\omega t}}{2}\left[\sqrt{H+\mathrm{i}\omega}\,\mathrm{erf}\sqrt{(H+\mathrm{i}\omega)t} + \frac{1}{\sqrt{t\pi}}\mathrm{e}^{-(H+\mathrm{i}\omega)t}\right] + \frac{\mathrm{Gr}}{H}\left[1-\frac{1}{\pi}\int_0^H \frac{\sqrt{H+x}}{x^{\frac{3}{2}}}\left[1-\mathrm{e}^{-tx}\right]\mathrm{d}x\right], \quad (17)$$

for $\mathrm{Pr}_{\mathrm{eff}} = 1$. The velocity $u(y,t)$, as well as the skin friction $\tau(t)$, consists of two parts. The first part, due to the oscillations of the plate, is not affected by thermal effects. The second part of the velocity, as well as the last term of the skin friction, are due to radiation and free convection currents.

3. Special Cases

Equations (12)–(14) provide exact analytical solutions for the fluid temperature and velocity for the unsteady hydromagnetic flow of an incompressible viscous electrically conducting fluid past an oscillating vertical plate when thermal effects and porosity are taken into consideration. In order to underline the influence of the corresponding parameters on the fluid motion, as well as for a check of results, it is worth pointing out different special cases of general solutions. It may be worthwhile to compare such a motion with the one where at least one of the above mentioned effects is absent.

3.1. Solution in the Absence of Radiation

In the absence of thermal radiation, i.e. in the pure convection case which numerically corresponds to $N_{\mathrm{r}} = 0$, the dimensionless temperature $\theta(y,t)$ takes the form

$$\theta(y,t) = \frac{2\sqrt{t}}{\sqrt{\mathrm{Pr}}}\left[\frac{1}{\sqrt{\pi}}\exp\left(-\frac{y^2\mathrm{Pr}}{4t}\right) - \frac{y\sqrt{\mathrm{Pr}}}{2\sqrt{t}}\,\mathrm{erf}\,c\left(\frac{y\sqrt{\mathrm{Pr}}}{2\sqrt{t}}\right)\right], \quad (18)$$

obtained in Chaudhary et. al. [14, Eq. (15)]. By now letting $N_{\mathrm{r}} = 0$ and $\omega = 0$ into (13) and (14), the velocity field obtained by Chaudhary et al. [14, Eqs. (16) or (17)] is recovered.

3.2. Solution in the Absence of Thermal, Magnetic, and Porous Effects

It is interesting to observe that in the absence of thermal effects, the Grashof number $\mathrm{Gr} = 0$ and the velocity field

$$u(y,t) = \frac{1}{4}\left[\mathrm{e}^{-\mathrm{i}\omega t}\left[\mathrm{e}^{-y\sqrt{H-\mathrm{i}\omega}}\,\mathrm{erf}\,c\left(\frac{y}{2\sqrt{t}} - \sqrt{(H-\mathrm{i}\omega)t}\right) + \mathrm{e}^{y\sqrt{H-\mathrm{i}\omega}}\,\mathrm{erf}\,c\left(\frac{y}{2\sqrt{t}} + \sqrt{(H-\mathrm{i}\omega)t}\right)\right] \quad (19)$$

$$+ \mathrm{e}^{\mathrm{i}\omega t}\left[\mathrm{e}^{-y\sqrt{H+\mathrm{i}\omega}}\,\mathrm{erf}\,c\left(\frac{y}{2\sqrt{t}}-\sqrt{(H+\mathrm{i}\omega)t}\right)\right.$$
$$\left.+\,\mathrm{e}^{y\sqrt{H+\mathrm{i}\omega}}\,\mathrm{erf}\,c\left(\frac{y}{2\sqrt{t}}+\sqrt{(H+\mathrm{i}\omega)t}\right)\right]\Bigg]$$

resulting from (13) or (14), corresponds to the MHD flow of an incompressible viscous fluid past an oscillating vertical infinite plate through a porous medium. For large time, the starting solution (19) tends to the steady state solution

$$u(y,t) = \mathrm{e}^{-\alpha y}\cos(\omega t - \beta y)\,, \tag{20}$$

where

$$\alpha^2 = \frac{\sqrt{H^2+\omega^2}+H}{2} \quad \text{and} \quad \beta^2 = \frac{\sqrt{H^2+\omega^2}-H}{2}\,.$$

The solutions corresponding to the MHD flow or through a porous medium are immediately obtained from (19) and (20) for $K \to \infty$, respectively $M = 0$. If $H \to 0$ (the magnetic and porous effects are also neglected), (19) and (20) reduce to the known solutions obtained by Erdogan [15, Eqs. (8) and (12)]. Finally making $\omega \to 0$ into (19) and (20), the solutions corresponding to the motion past an impulsively started infinite vertical plate are obtained.

4. Numerical Results and Discussion

In this note, the radiation and porosity effects on the MHD free convection flow of an incompressible viscous fluid past an infinite vertical oscillating plate with uniform heat flux are studied. The dimensionless governing partial differential equations are solved by the usual Laplace transform technique. Exact solutions for velocity and temperature are obtained in terms of the exponential and complementary error functions. They satisfy all imposed initial and boundary conditions and, in special cases, reduce to known solutions from the literature. Dimensional expressions for the skin friction, that is a measure of the shear stress on the plate, are also determined. In the absence of thermal radiation (when $q_r = 0$) and for $\omega \to 0$, all present solutions tend to those obtained by Chaudhary et al. [14].

In order to get physical insight and to understand the effects of different parameters in the problem, numerical computations are carried out for velocity, temperature, and skin friction for different values of pertinent parameters such as Grashof number Gr, radiation parameter N_r, magnetic parameter M, permeability parameter K, Prandtl number Pr, phase angle ωt, and time t. However, the Grashof number Gr in (13) and (14) can take positive, zero or negative values. Physically $\mathrm{Gr} < 0$ corresponds to an externally heated plate, $\mathrm{Gr} = 0$ corresponds to the absence of the free convection currents while $\mathrm{Gr} > 0$ corresponds to externally cooled plate [21]. The heating and cooling take place by setting up free convection current due to temperature and concentration gradient. In the case $\mathrm{Gr} = 0$, the velocity is independent of the Prandtl number Pr of the fluid and describes only hydromagnetic oscillations. This case will not be considered here, and we begin our graphs with the Grashof number.

Figure 1 clearly shows that the velocity increases with an increase of thermal Grashof number Gr in the case of cooling of the plate. For negative values of Gr, as expected, an opposite phenomenon appears. Figures 2–6 present the velocity profiles against y for air ($\mathrm{Pr} = 0.71$) due to the variations of $N_r, M, K, \omega t$, and time t for the case of heating ($\mathrm{Gr} < 0$) and cooling ($\mathrm{Gr} > 0$) of the plate. In Figure 2, the velocity profiles for different values of the radiation parameter N_r in cases of cooling and heating of the plate at $t = 0.2$ and $\omega t = \frac{\pi}{2}$ are presented. It is observed that the fluid velocity decreases with increasing values of N_r for the case of cooling of the plate. This is due to the fact that an increase in the radiation parameter N_r, for fixed k and T_∞, means an increase in the Rosseland mean absorbtion coefficient k^* [22]. A reverse effect is observed in the case of heating of the plate. Figure 3 illustrates the influence of the magnetic parameter M also in both cases of cooling and heating of the plate at $t = 0.2$. The velocity of the fluid decreases with an

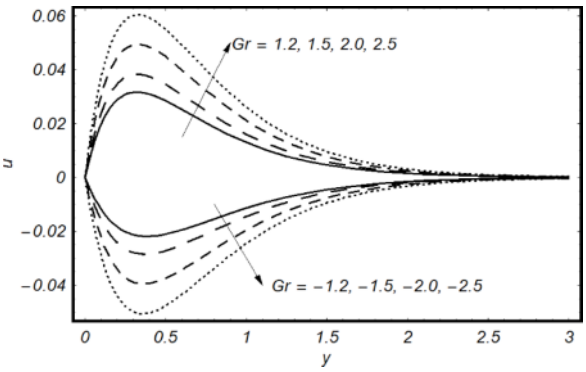

Fig. 1. Velocity profiles for different values of Gr with $t = 0.2$, $N_r = 1.2$, $M = 0.8$, $K = 1.4$, $\mathrm{Pr} = 0.71$, $\omega = 0.5$, and $\omega t = \frac{\pi}{2}$.

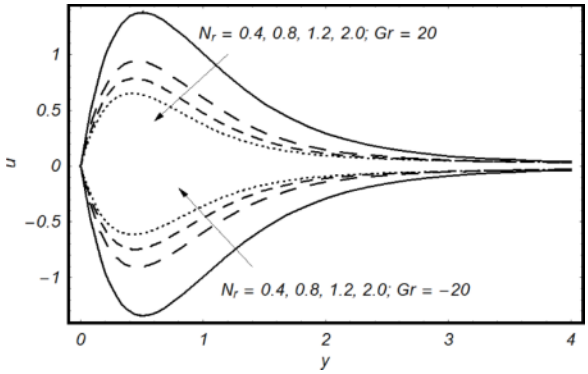

Fig. 2. Velocity profiles for different values of N_r with $t = 0.2, M = 0.8, K = 1.4, \Pr = 0.71$, $\omega = 0.5$, and $\omega t = \frac{\pi}{2}$.

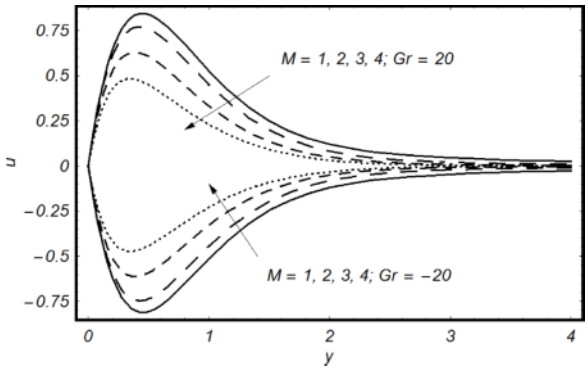

Fig. 3. Velocity profiles for different values of M with $t = 0.2, N_r = 2, K = 1.4, \Pr = 0.71, \omega = 0.5$, and $\omega t = \frac{\pi}{2}$.

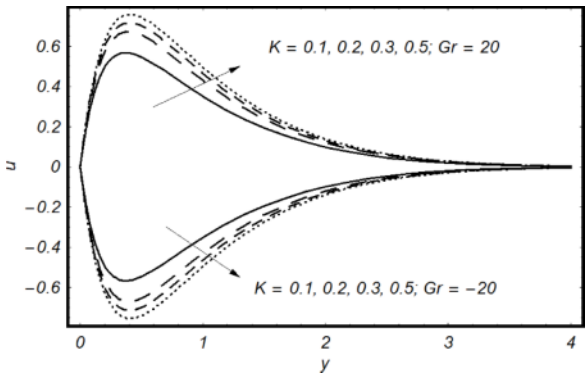

Fig. 4. Velocity profiles for different values of K with $t = 0.5, N_r = 2, M = 4, \Pr = 0.71, \omega = 0.2$, and $\omega t = \frac{\pi}{2}$.

increase of magnetic parameter M for the case of cooling of the plate. This is due to a resistive type force (Lorentz force) similar to drag force, which tends to resist the fluid flow and thus reduces its velocity. Clearly,

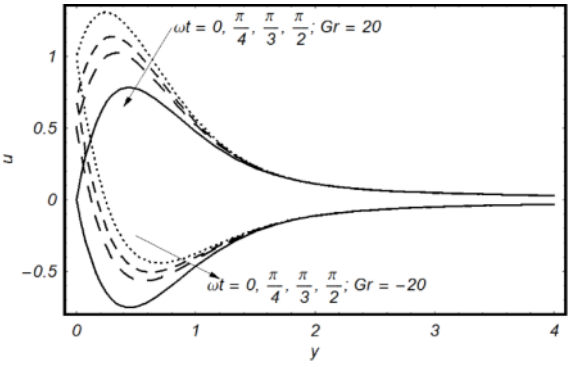

Fig. 5. Velocity profiles for different values of ωt with $t = 0.2, N_r = 1.2, M = 0.8, K = 1.4, \Pr = 0.71$, and $\omega = 0.5$.

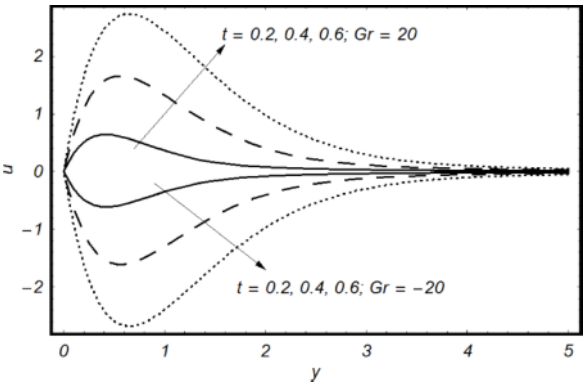

Fig. 6. Velocity profiles for different values of t with $N_r = 2, M = 1.4, K = 1.5, \Pr = 0.71, \omega = 0.5$, and $\omega t = \frac{\pi}{2}$.

a reverse effect is observed in the case of heating of the plate. In the case of cooling of the plate the velocity increases near the plate, becomes a maximum, and then decreases away from the plate asymptotically. The velocity profiles due to the variations in K (permeability parameter) are drawn in Figure 4. The velocity increases with an increase of the permeability parameter K for the case of cooling of the plate and decreases in the case of heating of the plate. This is due to the fact that the presence of a porous medium increases the resistance to flow. A reverse trend appears in the case of heating of the plate.

Figure 5 represents the velocity profiles due to the variations of the phase angle ωt in case of cooling and heating of the plate. The velocity of the fluid decreases with increasing the phase angle ωt for the case of cooling of the plate. A similar effect is also observed in the case of heating of the plate. It is clear from the figure that the velocity near the plate exceeds at the plate, i.e.

the velocity overshoot occurs. In Figure 6, the velocity profiles due to the variations in t (time) are displayed in cases of cooling and heating of the plate. It is observed that the velocity decreases with time for the case of cooling of the plate when the phase angle $\omega t = \frac{\pi}{2}$. A reverse effect is observed in the case of heating of the plate. In the case of cooling of the plate, the velocity increases near the surface of the plate, becomes a maximum, then decreases away from the plate and finally approaching zero asymptotically.

The temperature profiles of air (Pr = 0.71) are shown in Figure 7 and Figure 8 for different values of N_r and t. Figure 7 clearly shows that the temperature decreases with increasing values of radiation parameter N_r. When radiation is present, the thermal boundary layer was always found to thicken. This may be explained by the fact that radiation provides an additional means to diffuse energy. From Figure 8 it is observed that the temperature increases with increasing time in the presence of radiation. Furthermore, it is found that the thermal boundary layer thicken with increasing values of time. The effect of the Prandtl number Pr on the fluid temperature is analysed from Figure 9. It is noticed that the temperature decreases on increasing Pr, and the thickness of thermal boundary layer is greater for air (Pr = 0.71), and there is more uniform temperature distribution across the thermal boundary layer as compared to electrolytic solution (Pr = 1.0) and water (Pr = 7). The reason is that smaller values of Prandtl number are equivalent to increasing thermal conductivity and therefore heat is able to diffuse away from the heated surface more rapidly than for higher values of Prandtl number. Thus, the temperature falls more rapidly for water than air and electrolytic solution. The

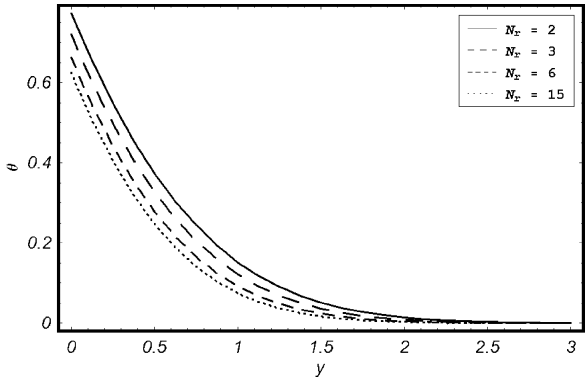

Fig. 7. Temperature profiles for different values of N_r with $t = 0.2$ and Pr = 0.71.

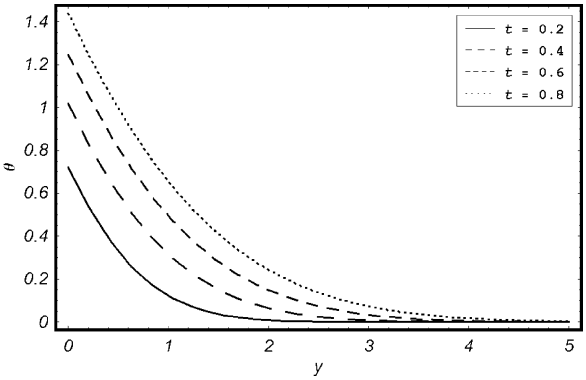

Fig. 8. Temperature profiles for different values of t with $N_r = 3$ and Pr = 0.71.

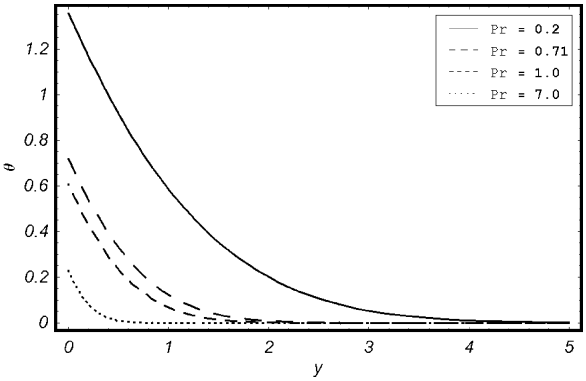

Fig. 9. Temperature profiles for different values of Pr with $t = 0.2$ and $N_r = 3$.

temperature is maximum near the plate and asymptotically approaches to zero in the free stream region.

The skin friction is presented in Figures 10 – 13. From Figure 10, it is clear that the skin friction decreases with an increase of thermal Grashof number Gr for both cooling and heating of the plate for time $t < 0.72$. But when $t > 0.72$, the skin friction increases with an increase of Gr for both cooling and heating of the plate. Figures 11 – 13 present the skin friction profiles for air (Pr = 0.71) due to variations of N_r, M, and K for the case of cooling (Gr > 0) and heating (Gr < 0) of the plate against time t and $\omega t = \frac{\pi}{2}$. In Figure 11, it is observed that the skin friction increases with increasing values of radiation parameter N_r for the case of cooling of the plate. An opposite phenomenon is observed in the case of heating of the plate. Figure 12 illustrates the influence of the magnetic parameter M in both cases of heating and cooling of the plate. The skin friction increases with an increase of M for the case of cooling

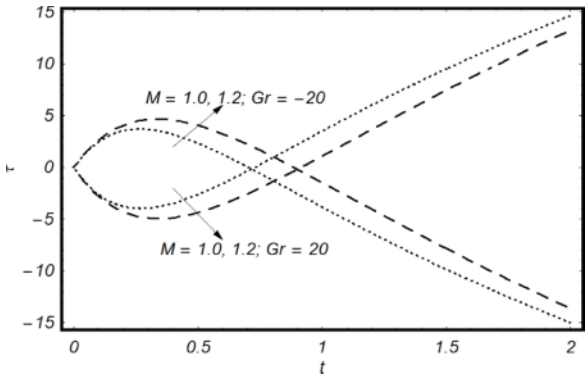

Fig. 10. Skin friction profiles for different values of M with $K = 1.4, \mathrm{Pr} = 0.71, N_{\mathrm{r}} = 2, \omega = 0.5$, and $\omega t = \frac{\pi}{2}$.

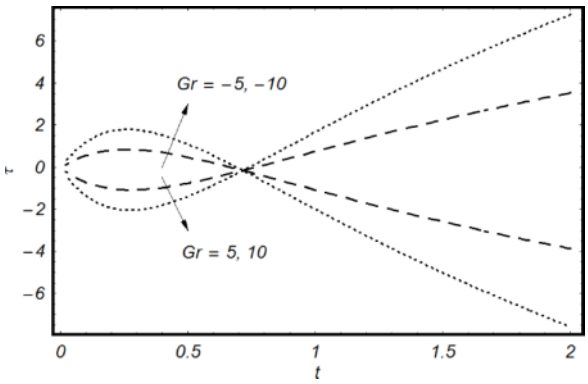

Fig. 12. Skin friction profiles for different values of Gr with $K = 1.4, \mathrm{Pr} = 0.71, M = 1.2, N_{\mathrm{r}} = 2$, $\omega = 0.5$, and $\omega t = \frac{\pi}{2}$.

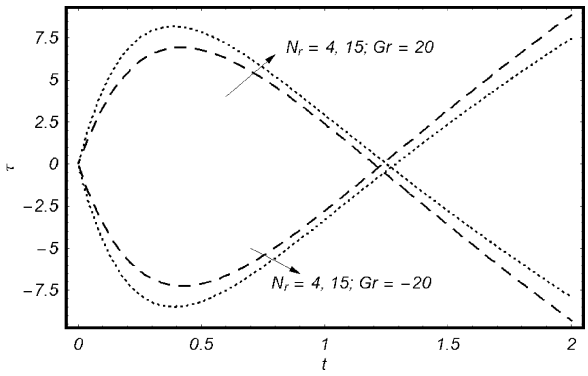

Fig. 11. Skin friction profiles for different values of N_{r} with $K = 1.4, \mathrm{Pr} = 0.71, M = 0.8, \omega = 0.5$, and $\omega t = \frac{\pi}{2}$.

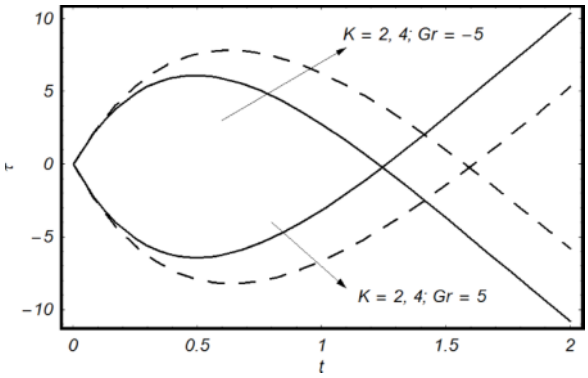

Fig. 13. Skin friction profiles for different values of K with $M = 1.2, N_{\mathrm{r}} = 2, \mathrm{Pr} = 0.71, \omega = 0.5$, and $\omega t = \frac{\pi}{2}$.

of the plate. Clearly, a reverse effect is observed in the case of heating of the plate. The skin friction profiles due to the variations in permeability parameter K are shown in Figure 13. The skin friction decreases with an increase of K in the case of cooling of the plate and increases for the case of heating of the plate.

5. Conclusions

In this study, we have analysed the governing equations for unsteady hydro-magnetic natural convective heat transfer flow of Boussinesq fluid past an oscillating vertical plate with uniform heat flux in a porous medium in the presence of radiative heat transfer. The governing equations are analytically solved by the Laplace transform technique. The cases of cooling and heating of the plate are considered corresponding to the Grashof number $\mathrm{Gr} > 0$ and $\mathrm{Gr} < 0$, respectively. The pertinent parameters bring to light the following effects on the velocity and temperature in case of cooling and heating of the plate:

(i) The Grashof number Gr accelerates the velocity of the fluid in case of cooling of the plate. A reverse effect is observed in the case of heating of the plate.

(ii) An increase in the radiation parameter N_{r} results in a decrease in velocity for $\mathrm{Gr} > 0$ and an increase when $\mathrm{Gr} < 0$. Also radiation parameter reduces the temperature of the fluid.

(iii) The magnetic parameter M retards the velocity of the fluid in case of cooling of the plate. Whereas, it enhances the velocity of the flow field in case of heating of the plate.

(iv) The phase angle ωt has a retarding effect on the fluid flow for both cooling and heating of the plate.

(v) The phase angle ωt has a retarding effect on the fluid flow for both cooling and heating of the plate.

(vi) The velocity of the fluid increases with time t in case of cooling and decreases in case of heating of the plate.
(vii) The temperature increases with increase in time t.
(viii) An increase in the Prandtl number Pr reduces the temperature of the fluid.
(ix) An increase in M or N_r results in an increase in the skin friction τ in case of cooling of the plate and a decrease in case of heating of the plate.
(x) The skin friction increases due to increase in K in case of heating and decreases in case of cooling of the plate.

Acknowledgement

The authors would like to acknowledge the Research Management Centre-UTM for the financial support through vote numbers 4F019 and 03J62 for this research.

[1] V. M. Soundalgekar, J. Heat Transfer **99**, 499 (1997).
[2] A. Raptis and A. K. Singh, Int. Commun. Heat Mass Transfer **10**, 313 (1983).
[3] A. K. Singh and N. Kumar, Astrophys. Space Sci. **98**, 245 (1984).
[4] V. M. Soundalgekar, Proc. Roy. Soc. A. **333**, 25 (1973).
[5] M. A. Mansour, Astrophys. Space Sci. **166**, 269 (1990).
[6] P. Chandrakala and P. N Bhaskar, Int. J. Appl. Mech. Eng. **14**, 349 (2009).
[7] A. Ishak, Heat Mass Transfer **46**, 147 (2009).
[8] A. Ishak, Meccanica **45**, 367 (2010).
[9] V. Rajesh and S. V. K. Varma, Int. J. Appl. Math. Mech. **6**, 39 (2010).
[10] M. Narahari and A. Ishak, J. Appl. Sci. **11**, 1096 (2011).
[11] G. S. Seth, Md. S. Ansari, and R. Nandkeolyar, Heat Mass Transfer **47**, 551 (2011).
[12] P. Chandrakala and P. N. Bhaskar, Int. J. Dyn. Fluids **7**, 9 (2011).
[13] P. Chandrakala, Int. J. Dyn. Fluids **7**, 1 (2011).
[14] R. C. Chaudhary, M. C. Goyal, and A. Jain, Matematicas: Ensenanza Universitaria **XVII**, 73 (2009).
[15] M. E. Erdogan, Int. J. Nonlin. Mech. **35**, 1 (2003).
[16] K. R Cramer and S. I Pai, Magnetofluid dynamics for engineers and applied physicists, McGraw-Hill, New York 1973.
[17] R. Siegel and J. H. Howell, Thermal Radiation Heat Transfer, 4th Edition, Taylor & Francis, London 2002.
[18] T. J. Chung, Computational Fluid Dynamics, Cambridge University Press, Cambridge 2002.
[19] U. N. Das, R. Deka and V. M. Soundalgekar, Forsch. Ingenieurwes. **60**, 284 (1994).
[20] E. Magyari and A. Pantokratoras, Int. Commun. Heat Mass Transfer **38**, 554 (2011).
[21] V. Rajesh, Int. J. Appl. Math. Mech. **6**, 1 (2010).
[22] M. Narahari, Weseas Transact. Heat Mass Transfer **1**, 21 (2010).